Deriving The Control-To-Output Transfer Function Of The Weinberg Converter

by Christophe Basso, Future Electronics, Toulouse, France

The Weinberg converter was first documented by Alan Weinberg in 1974 when he was with the European Space Agency.[1] The converter is a buck-derived current-fed push-pull topology and has gained popularity in space applications up to several kilowatts, owing to its robustness and almost ripple-free output current.

As with any switching converter intended to be operated in closed loop, the stabilization exercise starts with obtaining the control-to-output transfer function of the power supply. While searching the available literature, I have found several papers describing the small-signal response of this converter,[2, 3] but I could not either match their results with simulations in SIMPLIS or derive a useful expression from a long list of matrices. Finally, since this structure was not analyzed in my previous book on transfer functions,[4] I decided to take a look at its small-signal response here.

To begin we'll review the structure and operation of the Weinberg converter, focusing on a modified form which is commonly used. Next, we'll review Vorpérian's large-signal model of the PWM switch and discuss how it can be applied quickly to simulate both the dc and ac response of a converter in SPICE and SIMPLIS. We'll also discuss how that model can be used to derive a small-signal model of a converter, from which the desired control-to-output transfer function can be obtained.

With that as background, we'll derive a PWM switch model specific to the Weinberg converter, and generate a large-signal model of this converter, which we'll simulate in SPICE and SIMPLIS. With those simulations as reference points, we'll then derive the equivalent small-signal models of the PWM switch and Weinberg converter operated in voltage-mode control. Although this converter can also be operated in current-mode control, the complexity of the small-signal model in this mode becomes much greater and therefore the analysis becomes much longer. Hence, we'll stick with analysis of the Weinberg converter in voltage-mode.

Once we have the small-signal model of the converter (at the start of the section on "Small-Signal Analysis") we'll spend the remainder of the discussion applying fast analytical circuits techniques (FACTs) to derive the desired transfer function. Ultimately, we'll verify its correctness by checking the responses obtained for this transfer function in Mathcad with simulation results obtained in SIMPLIS.

The Weinberg Structure

The circuit associates the operating principle of forward and flyback converters, offering remarkable characteristics such as natural resilience against transformer saturation with an extremely low output ripple current. This converter represents a solution of choice for reliable low-voltage high-current applications such as those found in satellite power circuits.

The original implementation is known to suffer from voltage asymmetry in the primary-side power switch waveforms[5]. However, a modified version was patented in 1982 by Gordon (Ed) Bloom that corrects this problem.[6] This version is shown in Fig. 1 and I will derive its small-signal model.

The key point of this converter lies in the absence of a secondary-side inductor as one would expect with a push-pull implementation. Rather, a flyback transformer is inserted in series with the input. It magnetizes during the on-times of power switches Q1 and Q2 and releases energy to the output in their off-times. The reflected voltage across the transistors thus depends on the turns ratios of the flyback and push-pull transformers, respectively denoted as N_{fly} and N_{push} in the diagram. From reference [5] we have

$$V_{DS} = \begin{cases} 2V_{out}/N_{push} & \text{during } DT_{sw} \\ V_{in} + V_{out}/N_{fly} & \text{during } (1-D)T_{sw} \end{cases} \quad (1)$$

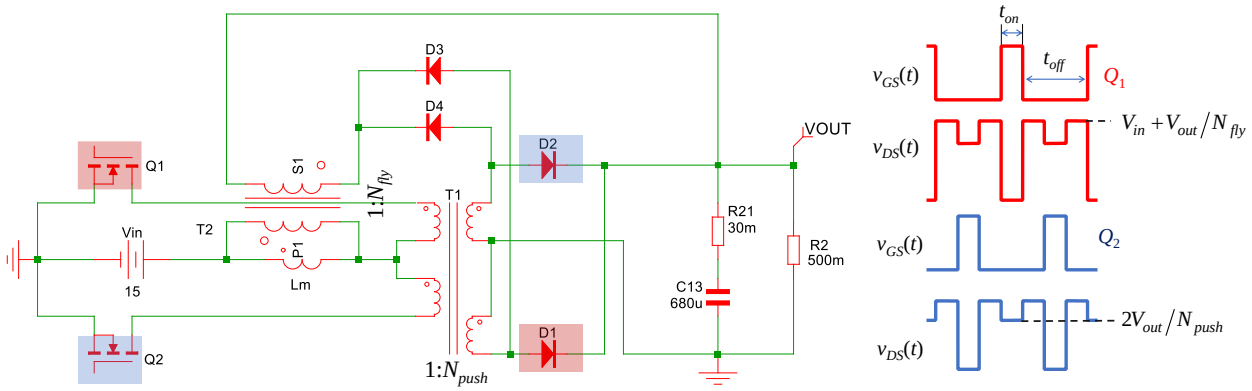

Fig. 1. The modified Weinberg converter combines a coupled inductor feeding a push-pull converter.

The current-fed structure brings another advantage according to reference [7]. A classical push-pull converter operated in voltage-mode control suffers from flux imbalance due to the possible mismatch in the voltage drops of Q_1 and Q_2. When this phenomenon happens, the transformer magnetic operating point drifts cycle-by-cycle and saturation occurs with all deleterious effects for the power switches. Current-mode control prevents this issue from happening and it is a well-known scheme for the classical voltage-fed push-pull converter.

The current-fed structure, on the other hand, is not immune to flux imbalance. However, when the transformer magnetic operating point runs away and approaches saturation, the increasing current absorbed by the switch at turn on, forces a larger drop at the transformer center tap owing to the series magnetizing inductance of the flyback transformer. This action naturally reduces the volt-seconds applied at the transformer half primary and prevents complete core saturation as would occur in a classical, voltage-fed converter. This inherent robustness against hard saturation has encouraged the adoption of the Weinberg converter in applications where reliability is key, as in the satellite industry for instance.

One major limitation of this converter is linked to the leakage inductances you can find in the two transformers. Switching waveforms captured in reference [8] clearly illustrate this problem. Mainly, these leakage inductances produce oscillations and spikes in the switching waveforms, and must be addressed in the design of the converter. But for the purposes of our ac analyses, the leakage inductances can be neglected, so their effects will not be included in the models to be derived.

The simulation results of an ideal circuit (no leakage inductances) are shown in Fig. 2 for a 5-V/10-A switching converter powered from a 15-V input source.

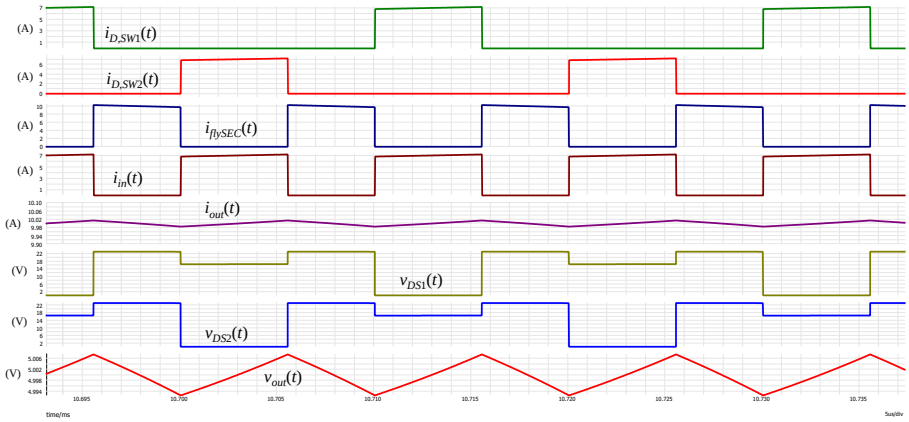

Fig. 2. The output current is almost constant, without ripple.

The PWM Switch At Work

The PWM switch model was documented by Vatché Vorpérian in 1986 and published in 1990 for the continuous and discontinuous conduction modes.[9,10] The three-terminal subcircuit is made of two simple *invariant* equations describing the *nonlinear* behavior of a switching cell made of active and passive switches (Fig. 3):

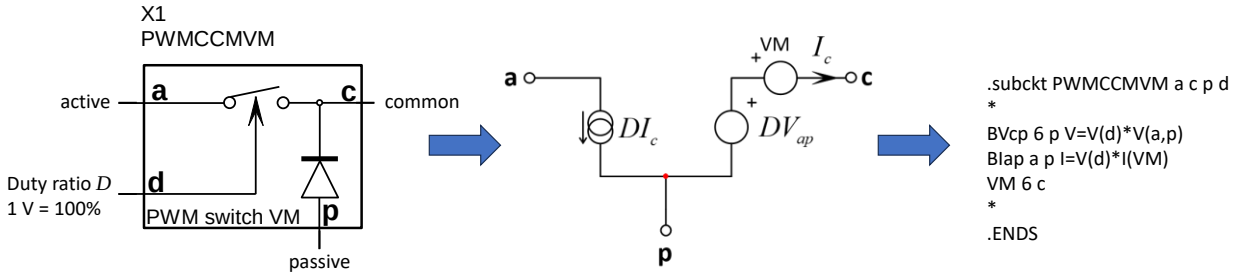

Fig. 3. The PWM switch model is unbeatable in terms of its simplicity. Its large-signal CCM model implements two simple equations. From the large-signal model, SPICE generates the small-signal model and provides ac analysis.

The term invariant refers to the fact that the mathematical relationships linking voltages and currents of the three terminals, do not change with respect to the topology in which the PWM switch is inserted. The idea is the same as with a transistor model: identify the core switching cell in the converter, insert the PWM switch respecting voltage and current polarities in lieu of the original symbols (switch and diode) and, voilà, it becomes possible to extract dc and ac responses with a simulator.

If you carry on and implement the small-signal model of the PWM switch through your analysis, then you now have an entirely linear circuit for which you can apply classical analysis tools such as Laplace transform and extract the transfer function of your choice.

SPICE being a linear solver in essence, you can use the non-linear model in your switching topology and immediately obtain the dc and ac responses. This is what is shown on the left side of Fig. 4 for a voltage-mode CCM buck converter. The duty ratio *D* is set to 51% by the 510-mV dc bias applied to the control input while an ac stimulus is superimposed over it. The ac response shows a damped second-order behavior with a zero brought by the output capacitor equivalent series resistance r_C.

As explained, if you want to derive a given transfer function, for instance the control-to-output linking V_{out} to *D*, then you have to resort to a linearized version as illustrated by the diagram on the lower left of Fig. 4. The ac responses in both cases are rigorously identical, confirming the validity of the small-signal model.

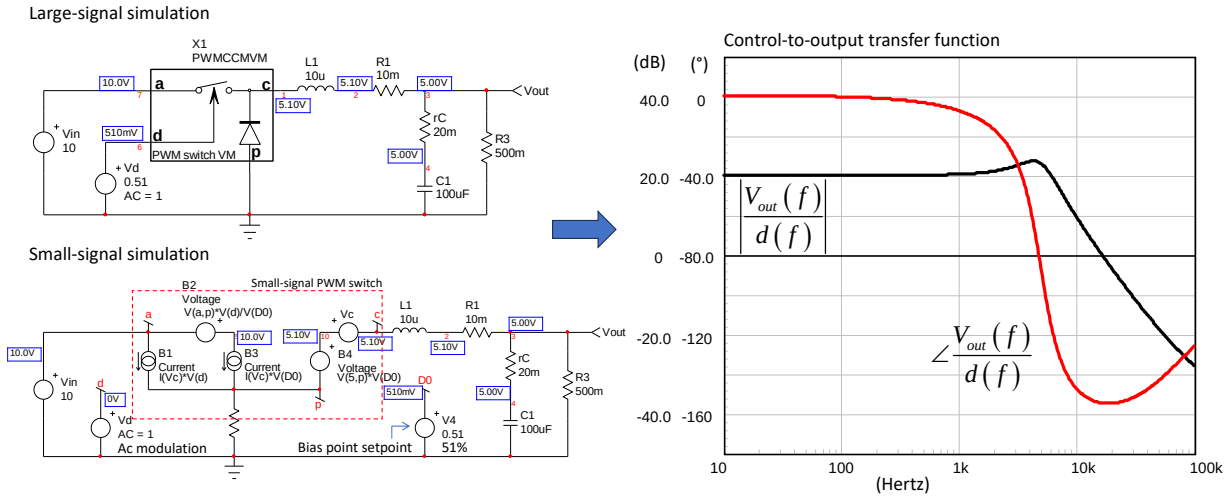

Fig. 4. SPICE will linearize the circuit and deliver a dc operating point followed by a small-signal response.

Modeling The Weinberg Converter

If the PWM switch is easily identified in classical structures such as the buck, the boost, or the buck-boost converters, some structures require more or less complicated manipulations to insert it properly. The Weinberg converter featuring the PWM switch model, luckily, has already been drawn by Vatché Vorpérian during a seminar he hold in Toulouse, back in 2004.[11] However, no explanation was given on how to get there and no transfer function derivation was provided in the teaching material. So we'll have to do some analysis to see how that model was obtained.

The starting point for building the equivalent circuit, consists of drawing the converter during the on- and off-times, involving the active power switches. Then, you have to find an arrangement—sometimes via added components such as a transformer, sources or even a second PWM switch—which satisfies both circuits when *averaged* by the PWM switch.

From the circuit shown in Fig. 1, we consider transistor Q_2 to be turned on. The primary mesh involves the flyback magnetizing inductance L_p whose current I_1 circulates in the secondary, scaled by the push-pull transformer turns ratio denoted as $1:N_{push}$. D_2 conducts this current and feeds the capacitor with the load resistance. In this mode, we can conveniently "push" the source and the magnetizing inductance to the secondary side via the push-pull transformer turns ratio. Fig. 5 shows this equivalent circuit which is valid during the on-time or DT_{sw}.

When Q_2 opens, the energy stored in the magnetizing inductance transfers to the secondary and D_2 blocks. The primary-side current I_1, now scaled by the flyback transformer ratio $1:N_{fly}$, feeds the resistance and the capacitor via diode D_4 which conducts.

Looking back at the right-side circuit in Fig. 5, the input source $V_{in}N_{push}$ is disconnected and an inductance still feeds the output *RC* network. Unfortunately, this inductance is no longer the one we had during the on-time but is the magnetizing inductance pushed to the secondary side of the flyback transformer. The challenge now is to find a way to reuse the Fig. 5 inductance which equals $L_p N_{push}^2$ during the on-time, and transform it into $L_p N_{fly}^2$ during the off-time.

The solution consists of adding a transformer with the correct turns ratio configuration as illustrated in Fig. 6. If you follow the expressions that I have detailed, you realize that the original inductance from the on-time is now

reflected through the added transformer turns ratio—which now depends on both flyback and push-pull magnetics—and transforms into the correct value of $L_p N_{fly}^2$ during the off-time.

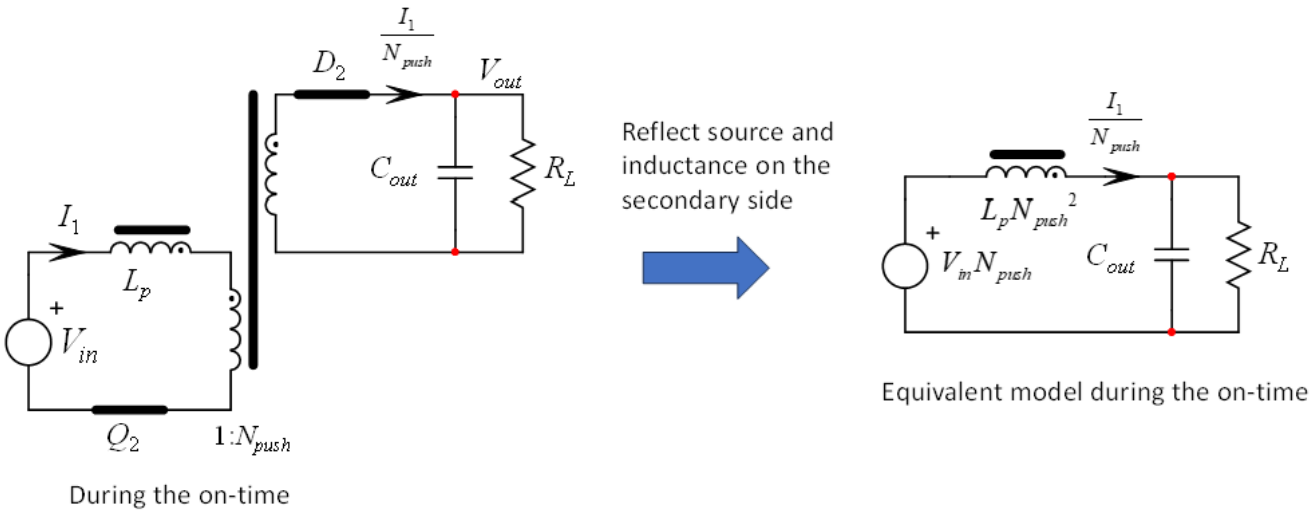

Fig. 5. When Q_2 turns on, current I_1 flows in the primary and scales by the transformer turns ratio to feed the load and the output capacitor. The magnetizing inductance of the push-pull transformer is ignored in this circuit.

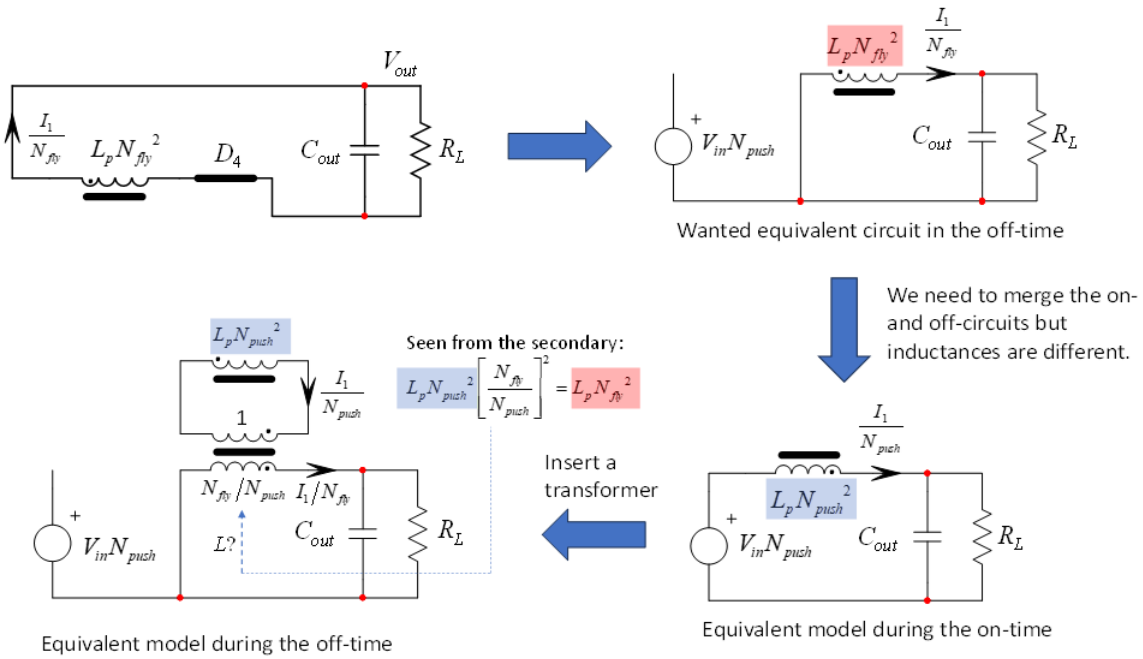

Fig. 6. Adding a transformer across the on-time reflected magnetizing inductance, satisfies the equivalent circuit equations during the off-time.

From there, I have gathered these equivalent circuits around the PWM switch and, in Fig. 7, you can see the final circuit we will use for the Weinberg averaged model. I have highlighted the network involved during the on-time in red, while the blue color corresponds to the off-time. As such, this model nicely merges the two events and we are ready to use it.

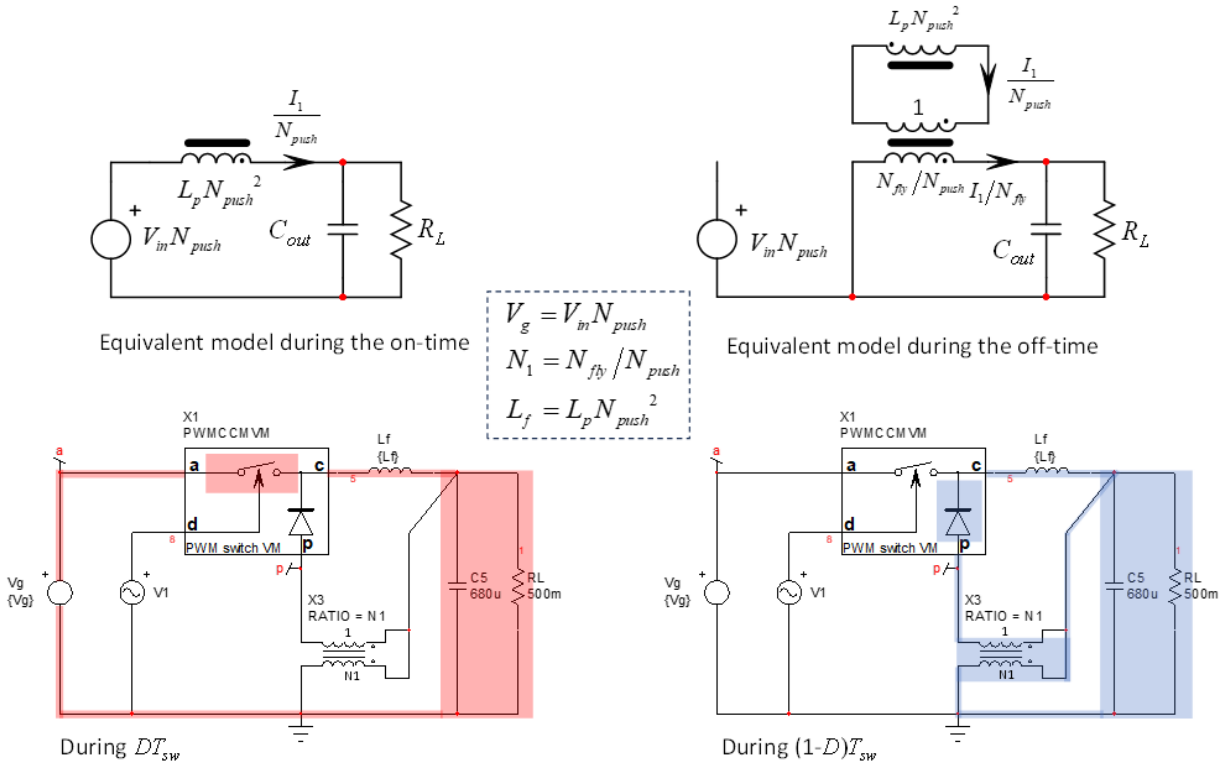

Fig. 7. The PWM switch correctly involves the two on- and off-circuits.

Before we proceed, we must check the dc bias points and the ac response of this circuit (Fig. 8) versus a cycle-by-cycle simulation with SIMPLIS for example (Fig. 9). The converter includes a pulse-width modulator featuring a 2-V peak ramp (attenuation of 6 dB) and is designed to deliver 5 V. Both turns ratios are identical in this particular example but we will later see how choosing different ones affects the converter's dynamics. The left-side macro in Fig. 8 computes all equivalent components and passes parameters to the subcircuits. This is extremely convenient and the same is possible with SIMPLIS.

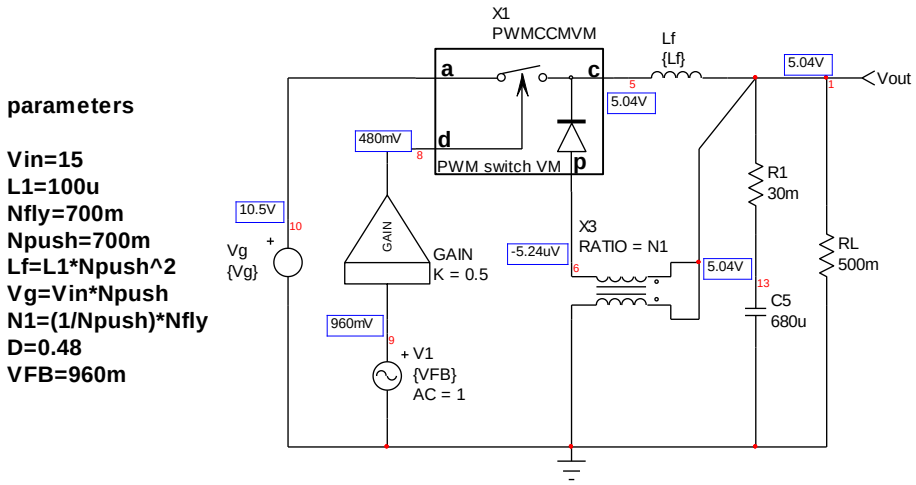

Fig. 8. This is the large-signal averaged model of the Weinberg converter.

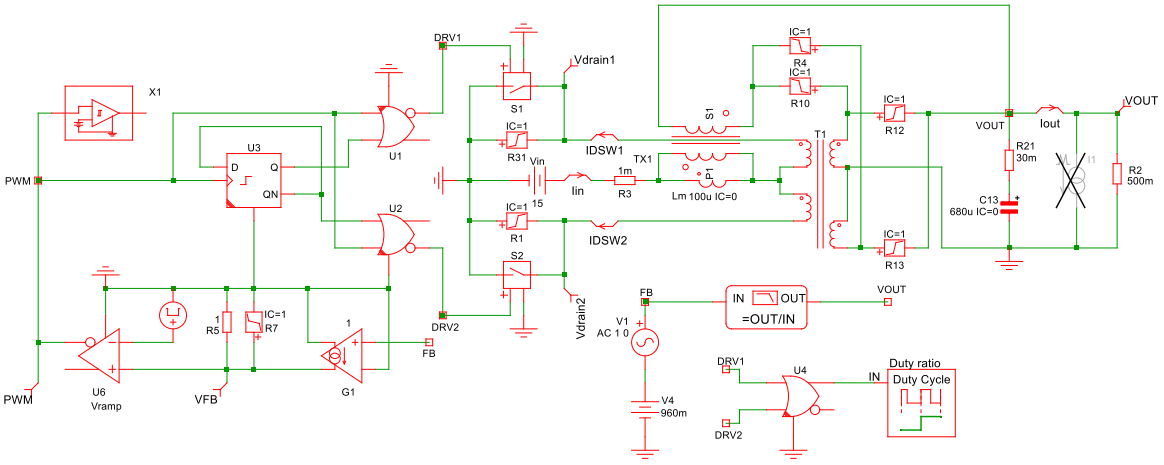

Fig. 9. The cycle-by-cycle simulation involves a 100-kHz clock and some logic to generate the control signals.

Fig. 10 confirms the 5-V output from both simulations and you can see how the ac responses in magnitude and phase perfectly superimpose on each other. A comprehensive check would obviously involve more tests such as input and output impedance or source-to-output transfer functions for instance but they will not be presented here as it is the control-to-output dynamic response of the power stage that we want.

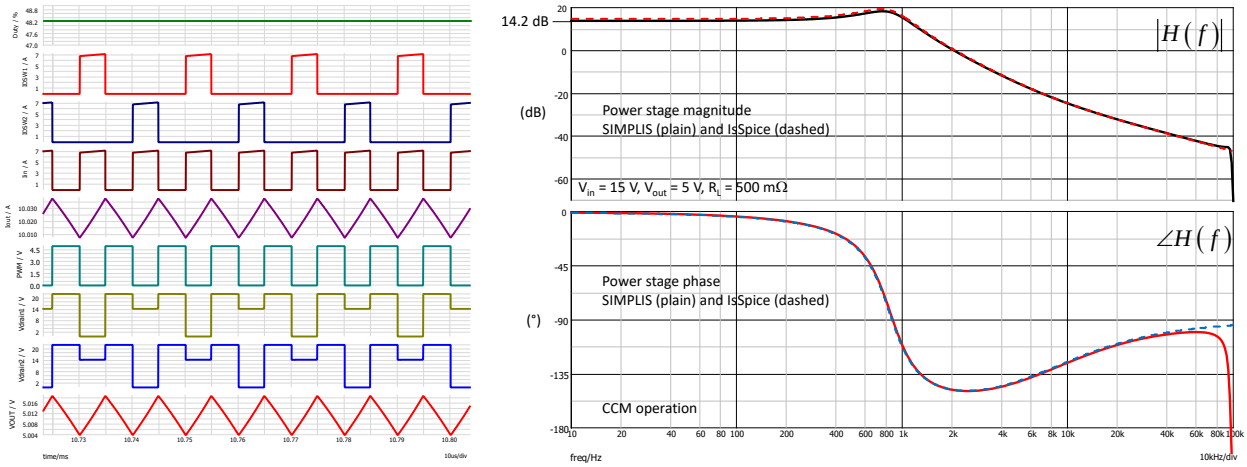

Fig. 10. The dc operating point (left) and the ac response (right) from SPICE and SIMPLIS are in excellent agreement.

Operating Point Analysis

Before proceeding with the small-signal response, we have to determine the dc transfer characteristics of the converter. Similarly, the small-signal model will require values for the voltage between terminals *a* and *p* of the PWM switch as well as the current I_c leaving terminal *c*.

Fig. 11 shows the circuit in dc conditions where the inductance is replaced by a wire and the capacitor is open-circuited. In this illustration, I purposely adopted different transformer turns ratios for N_{fly} and N_{push} which lead to the 3.7-V level. I also tested $N_{fly} = N_{push}$ and V_{out} = 5 V for the completeness of the sanity check.

From the configuration, we can see that V_{out} is applied at the secondary side of the extra transformer. The reflected value appears across terminals *c* and *p* leading to:

$$DV_{ap} = \frac{V_{out}}{N_1} \tag{2}$$

Extracting V_{ap} gives

$$V_{ap} = \frac{V_{out}}{DN_1} = \frac{V_{out}}{D}\frac{N_{push}}{N_{fly}} \tag{3}$$

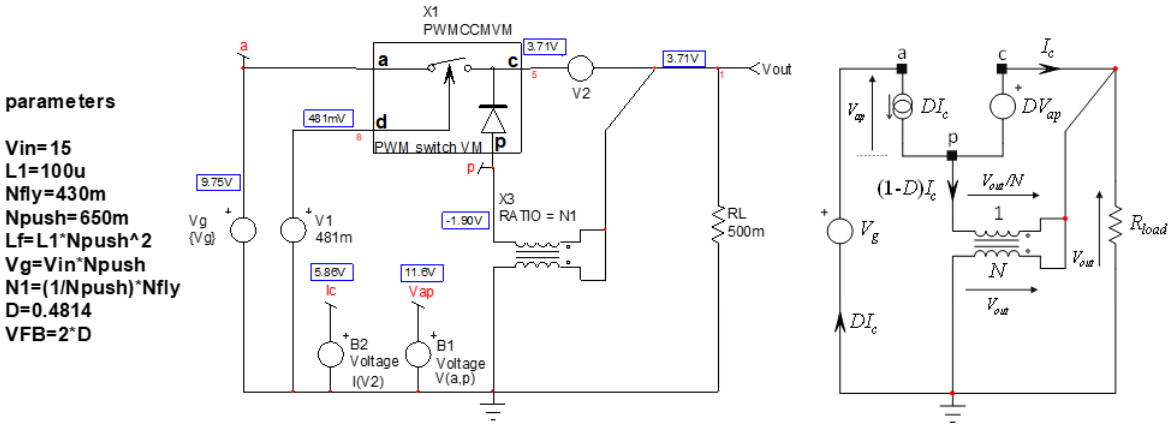

Fig. 11. The dc transfer characteristic is only a few equations away.

To determine the output voltage, write the mesh involving the source V_g, the voltage V_{ap} we have just derived, the primary-side voltage of the transformer and the output voltage:

$$V_g - \frac{V_{out}}{D}\frac{N_{push}}{N_{fly}} + V_{out}\frac{N_{push}}{N_{fly}} = V_{out} \tag{4}$$

Solve for V_{out}, replace V_g by $V_{in}N_{push}$, factor and rearrange:

$$V_{out} = V_{in}\frac{N_{fly}D}{1 + D\left(\frac{N_{fly}}{N_{push}} - 1\right)} \tag{5}$$

If we extract the duty ratio *D*, we have:

$$D = \frac{1}{1 - \frac{N_{fly}}{N_{push}} + N_{fly}\frac{V_{in}}{V_{out}}} \tag{6}$$

To determine the current I_c leaving terminal *c*, we consider a 100% efficiency and we equate the power delivered by the source V_g with that absorbed by the load resistance R_{load}:

$$V_g DI_c = \frac{V_{out}^2}{R_{load}} \tag{7}$$

We can extract I_c and rearrange the expression:

$$I_c = \frac{V_{out}^2}{DV_g R_{load}} = \frac{V_{out}^2}{N_{push} DV_{in} R_{load}} \tag{8}$$

Once these expressions are entered in a Mathcad sheet, they confirm the values labeled as operating points in the left-side circuit of Fig. 11:

$V_{in} := 15V$ $V_{out} := 3.70942V$ $R_{load} := 0.5\Omega$

$N_{fly} := 0.430$ $N_{push} := 0.65$ $V_g := V_{in} \cdot N_{push} = 9.75V$

$$D := \frac{1}{1 - \frac{N_{fly}}{N_{push}} + N_{fly} \cdot \frac{V_{in}}{V_{out}}} = 48.14\%$$

$$V_{out} := \frac{D \cdot N_{fly} \cdot V_{in}}{1 + D \cdot \left(\frac{N_{fly}}{N_{push}} - 1 \right)} = 3.709V$$

$$I_c := \frac{V_{out}^2}{N_{push} \cdot D \cdot V_{in} \cdot R_{load}} = 5.863A$$

$$V_{ap} := \frac{V_{out}}{D} \cdot \frac{N_{push}}{N_{fly}} = 11.648V$$

Fig. 12. These Mathcad results confirm the dc bias point calculated by SPICE in Fig. 11.

Quasi-Static Gain Of The Weinberg Converter

From the dc transfer characteristic derived in equation (5), we can obtain the quasi-static gain H_0 of this converter: if D changes a little bit, how does it affect the output voltage V_{out}? In other words, we can determine the *sensitivity* of $V_{out}(D)$ to D, the duty ratio. Mathematically, we perform a *differentiation* of V_{out} with respect to D:

$$\frac{d}{dD} V_{out}(D) = \frac{d}{dD} \left[V_{in} \frac{N_{fly} D}{1 + D\left(\frac{N_{fly}}{N_{push}} - 1 \right)} \right] = \frac{N_{fly} N_{push}^2 V_{in}}{\left[\left(N_{fly} - N_{push} \right) D + N_{push} \right]^2} \tag{9}$$

If we now include the PWM gain $G_{PWM} = 1/V_p$, with V_p the peak of the sawtooth, we have the complete dc gain expression:

$$H_0 = \frac{d}{dD} V_{out}(D) \cdot G_{PWM} = \frac{1}{V_p} \frac{N_{fly} N_{push}^2 V_{in}}{\left[\left(N_{fly} - N_{push} \right) D + N_{push} \right]^2} \tag{10}$$

I have checked this expression with a .TF SPICE statement used in the Fig. 11 circuit, this time delivering 5 V from the 15-V input source. As shown in Fig. 13, we are good to go.

$V_{in} := 15V$ $V_{out} := 5V$ $R_{load} := 0.5\Omega$ $V_p := 2V$

$N_{fly} := 0.7$ $N_{push} := 0.7$ $V_g := V_{in} \cdot N_{push} = 10.5V$

$$D := \frac{1}{1 - \frac{N_{fly}}{N_{push}} + N_{fly} \cdot \frac{V_{in}}{V_{out}}} = 47.619\% \qquad V_{out} := \frac{D \cdot N_{fly} \cdot V_{in}}{1 + D \cdot \left(\frac{N_{fly}}{N_{push}} - 1 \right)} = 5V$$

$$\frac{d}{dD}\left[\frac{D \cdot N_{fly} \cdot V_{in}}{1 + D \cdot \left(\frac{N_{fly}}{N_{push}} - 1 \right)} \right] = \frac{N_{fly} \cdot N_{push}^{\,2} \cdot V_{in}}{\left(N_{push} + D \cdot N_{fly} - D \cdot N_{push} \right)^2}$$

$$H_0 := \frac{1}{V_p} \cdot \frac{N_{fly} \cdot N_{push}^{\,2} \cdot V_{in}}{\left(N_{push} + D \cdot N_{fly} - D \cdot N_{push} \right)^2} = 5.25 \qquad 20 \cdot \log\left(H_0 \right) = 14.403 \quad dB$$

V_{out} D

```
.TF V(1) V1
***** SMALL SIGNAL DC TRANSFER FUNCTION

    output_impedance_at_V(1)        2.743768e-007
    v1#Input_impedance              1.000000e+020
    Transfer_function               5.250002e+000

Total run time:  0.050 seconds.
```

Fig. 13. The dc gain derived in equation 10 produces the result in Mathcad (on the left), which is confirmed by the SPICE simulation (on the lower right).

Small-Signal Analysis

The quasi-static gain determination represents the first step in deriving the complete transfer function of this converter. The next step is to draw the small-signal equivalent circuit from the large-signal circuit of Fig. 8 and find the transfer function you want. Once the linearized PWM switch subcircuit of Fig. 4 is inserted, the network updates to that of Fig. 14 and includes controlled voltage and current sources. In this picture, the term D_0 refers to the static duty ratio (the setpoint) while d corresponds to the ac input, our stimulus.

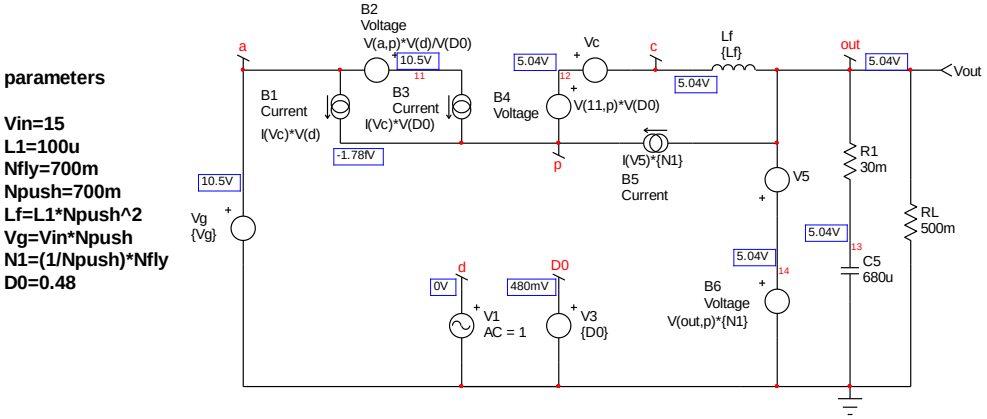

Fig. 14. When the small-signal PWM switch is first inserted, the electrical diagram can seem rather difficult to follow.

When you insert the PWM switch into the original electrical diagram, you usually end up with many components and sources that are very often not connected in a meaningful way, with floating nodes and so on. I recommend that you take time to rearrange the circuit elements in a way that allows you to follow the flow and see how the sources and nodes interact together.

For me, the arrangement that makes sense in this case is shown in Fig. 15 in which I have zeroed the input source V_g since it is 0 V ac for the control-to-output transfer function we want. During the steps taken in rearranging the original circuit, it is very important to run sanity checks time to time, by comparing the dc and ac responses of a given intermediate diagram with those of the founding circuit of Fig. 8. Any significant deviation indicates an error or an incorrect simplification. I recommend going through these steps to make sure you analyze a sound circuit in the end.

There are two energy-storing elements in Fig. 15—with independent state variables—making this circuit a second-order network. The denominator $D(s)$ is thus expressed by a second-degree polynomial:

$$D(s) = 1 + sb_1 + s^2 b_2 \qquad (11)$$

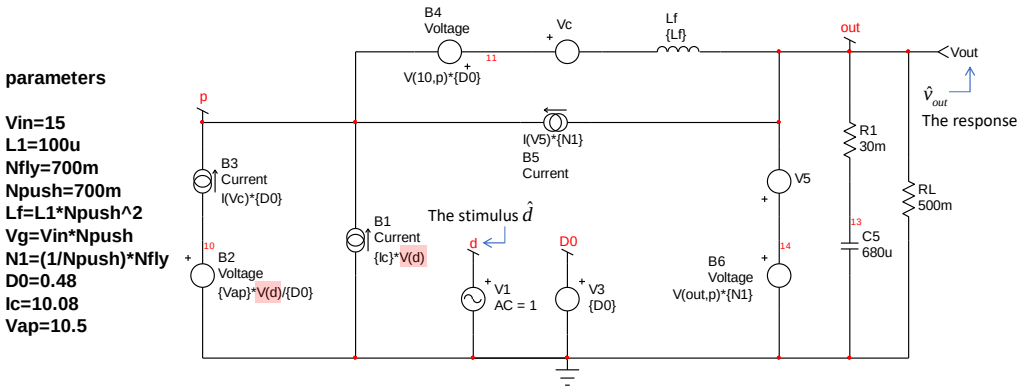

Fig. 15. This is the small-signal equivalent circuit of the CCM Weinberg converter operated in voltage-mode control.

We are going to calculate coefficients b_1 and b_2 with the fast analytical circuits techniques or FACTs that I have extensively applied in reference [4]. The poles are studied with a zeroed stimulus, meaning $\hat{d} = 0$. Voltage and current sources controlled by $\hat{d}$ will then respectively be replaced by a wire or open-circuited. The new network, after simplification, is shown in Fig. 16:

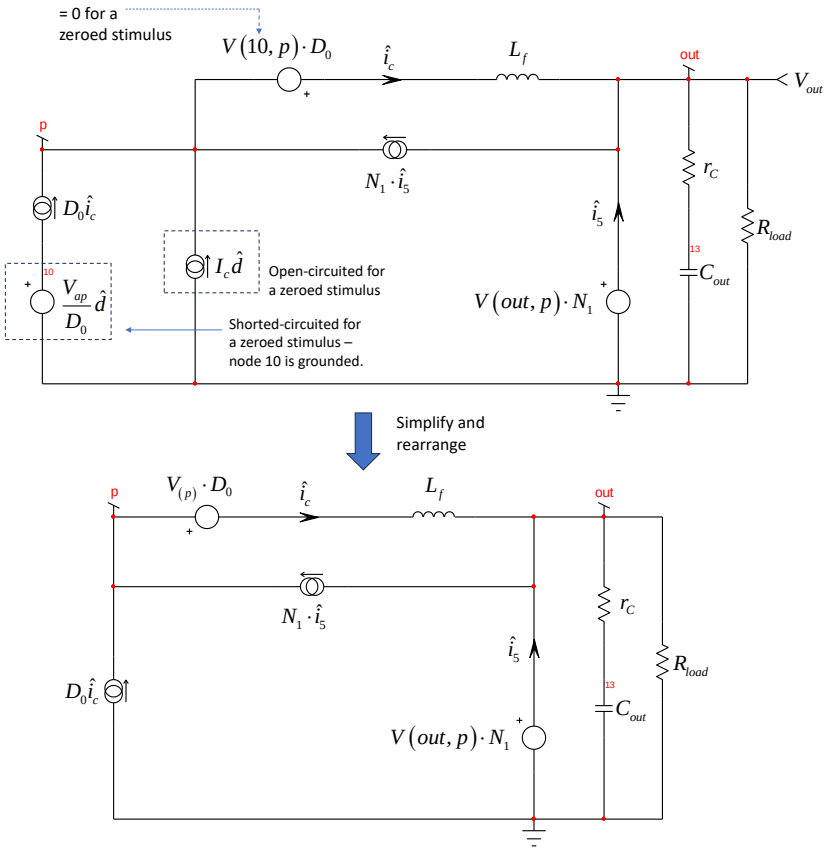

Fig. 16. Once the stimulus is turned off, the circuit greatly simplifies.

We start by setting C_{out} in its dc state while we determine the resistance R driving the inductor. We are looking at Fig. 17. Inspection is not possible here and you have to install a test generator injecting a current I_T. The exercise now consists of expressing voltage V_T which will lead us the resistance we want for the time constant: $R = V_T / I_T$.

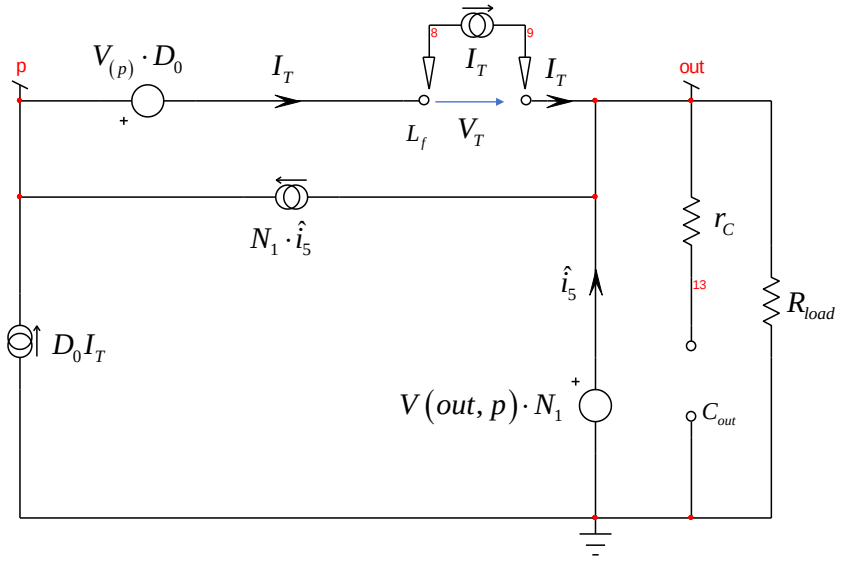

Fig. 17. The capacitor is placed in its dc state (and open circuit) and you determine the resistance R offered by the inductor's connecting terminals.

Current i_5 is quickly identified as

$$i_5 = \frac{I_T (1 - D_0)}{N_1} \tag{12}$$

Voltage V_T depends on left and right potentials of current source I_T:

$$V_T = V_{(out)} - V_{(p)} (1 - D_0) \tag{13}$$

The output voltage depends on the current flowing in the load resistance:

$$V_{(out)} = R_{load} (I_T - N_1 i_5 + i_5) \tag{14}$$

V_{out} also appears across the lower right-side source:

$$V_{(out)} = V_{(out)} N_1 - V_{(p)} N_1 \tag{15}$$

Combining the above equations gives us the resistance we need:

$$R = \frac{V_T}{I_T} = \frac{R_{load}\left(D_0 N_1 - D_0 + 1\right)^2}{N_1^{\,2}} \tag{16}$$

It leads us to the first time constant involving L_f:

$$\tau_1 = \frac{L_f}{R} = \frac{L_f N_1^{\,2}}{R_{load}\left(D_0 N_1 - D_0 + 1\right)^2} \tag{17}$$

For the second time constant involving C_{out}, L_f is now placed in its dc state (a short circuit) and the network to study updates to that of Fig. 18.

Since the resistance we want is that "seen" from C_{out}'s terminals, it naturally involves r_C in series. Therefore, for the sake of simplifying the analysis, we can temporarily remove r_C and determine an intermediate resistance. The final result will thus be r_C added to this intermediate result. Observing the circuit, we can see that

$$V_T = V_{(out)} \tag{18}$$

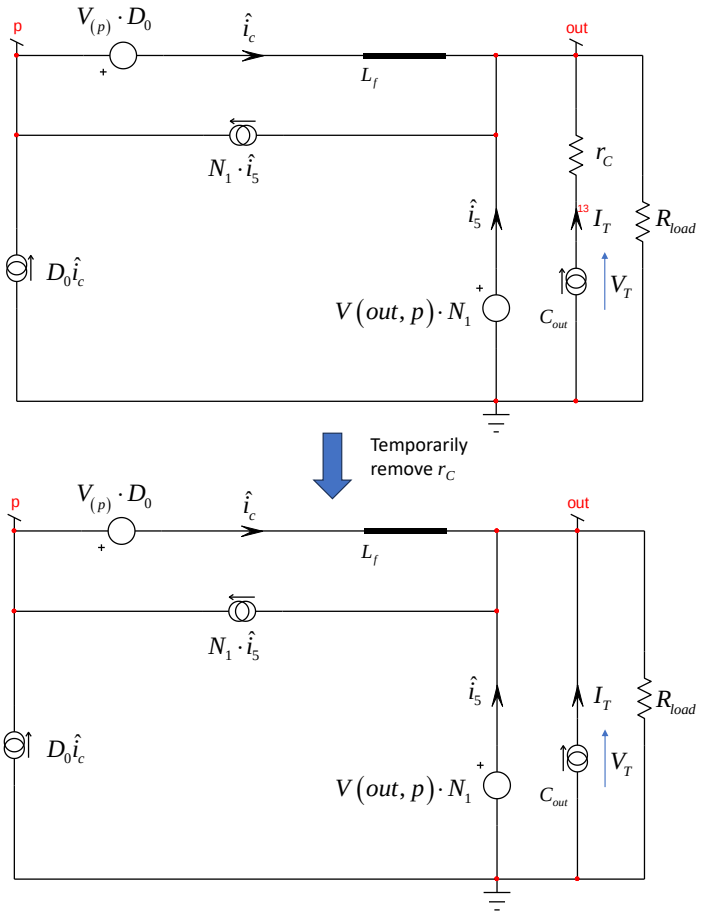

Fig. 18. The inductor is now placed in its dc state (a short circuit) while we determine the resistance R driving the capacitor.

The output voltage is also present across the voltage source creating i_5:

$$V_{(out)} = V_{(out)}N_1 - V_{(p)}N_1 \tag{19}$$

From this expression, extract the voltage at node *p*:

$$V_{(p)} = -\frac{V_{(out)} - N_1 V_{(out)}}{N_1} \tag{20}$$

Another expression leads to the voltage at node *p*:

$$V_{(p)} - V_{(p)}D_0 = V_{(out)} \tag{21}$$

From which we obtain

$$V_{(p)} = \frac{V_{(out)}}{1 - D_0} \tag{22}$$

We can now equate (22) with (20) to find out that $V_{(out)} = V_T = 0$ V, hence $R = 0\ \Omega$ for this intermediate result. The only resistance seen by capacitor C_{out} is thus r_C, leading to the second time constant:

$$\tau_2 = r_C C_{out} \tag{23}$$

With these two time constants, we can assemble coefficient b_1:

$$b_1 = \tau_1 + \tau_2 = \frac{L_f N_1^{\,2}}{R_{load}\left(D_0 N_1 - D_0 + 1\right)^2} + r_C C_{out} \tag{24}$$

We now determine the resistance *R* driving C_{out} while L_f is placed in its high-frequency state (an open circuit). The corresponding time constant will be denoted τ_2^1.[4] Fig. 19 shows the results with one simplification owing to the zeroing of current $\hat{\imath}_c$, consequence of opening L_f:

$$V_{(out)}N_1 - V_{(p)}N_1 = V_{(out)} \tag{25}$$

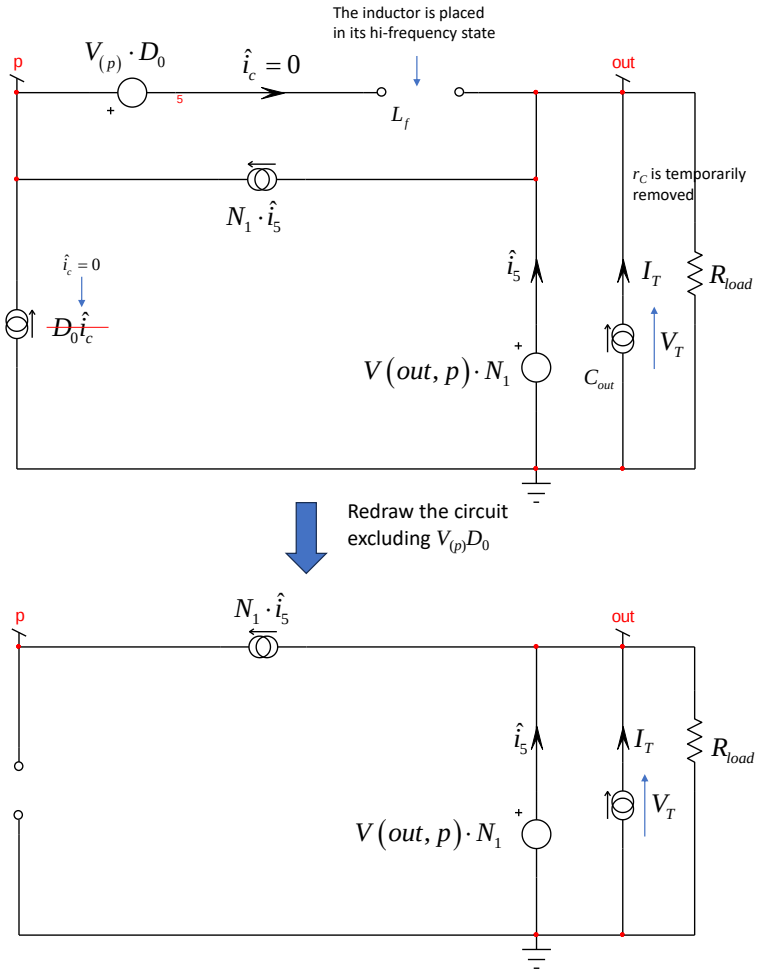

Fig. 19. The inductor is placed in its high-frequency state (an open circuit) while we determine the resistance R driving the capacitor. r_C is again temporarily omitted for this intermediate result.

Considering the opening of the circuit at node *p*, there is no current imposed by the current source which should be zero also. Therefore, $i_5 = 0$ A. The only resistance in which I_T flows is R_{load}, leading to the time constant we want after r_C is added to this intermediate result:

$$\tau_2^1 = C_{out}\left(r_C + R_{load}\right) \tag{26}$$

Combining the above definition with (17), completes the process for determining coefficient b_2:

$$b_2 = \tau_1\tau_2^1 = \frac{L_f N_1^2}{R_{load}\left(D_0 N_1 - D_0 + 1\right)^2} C_{out}\left(r_C + R_{load}\right) \tag{27}$$

We now have all we need to express the denominator:

$$D(s) = 1 + b_1 s + b_2 s^2 = 1 + s\left(\tau_1 + \tau_2\right) + s^2\tau_1\tau_2^1 \tag{28}$$

Replacing the time constants by their definitions leads to

$$D(s)=1+s\left(\frac{L_f N_1^2}{R_{load}\left(D_0N_1-D_0+1\right)^2}+r_C C_{out}\right)+s^2\frac{L_f N_1^2}{R_{load}\left(D_0N_1-D_0+1\right)^2}C_{out}\left(r_C+R_{load}\right) \quad (29)$$

The important thing is now to reshape this expression under a normalized second-order polynomial form to reveal a quality factor *Q* and a resonant frequency ω_0. This is what I have done in Fig. 20.

$$D(s)=1+sb_1+s^2b_2$$

$$D(s)=1+\frac{s}{\omega_0 Q}+\left(\frac{s}{\omega_0}\right)^2 \rightarrow \omega_0=\frac{1}{\sqrt{b_2}} \quad Q=\frac{\sqrt{b_2}}{b_1}$$

$$\omega_0=\frac{1}{\sqrt{\frac{L_f N_1^2}{R_{load}\left(D_0N_1-D_0+1\right)^2}C_{out}\left(r_C+R_{load}\right)}} \qquad Q=\frac{\sqrt{\frac{L_f N_1^2}{R_{load}\left(D_0N_1-D_0+1\right)^2}C_{out}\left(r_C+R_{load}\right)}}{\frac{L_f N_1^2}{R_{load}\left(D_0N_1-D_0+1\right)^2}+r_C C_{out}}$$

If we neglect the ESR contribution, $r_C \ll R_{load}$:

$$\omega_0 \approx \frac{\left(N_1-1\right)D_0+1}{N_1}\frac{1}{\sqrt{L_f C_{out}}} \qquad Q \approx \frac{R_{load}\left(N_1-1\right)D_0+1}{N_1}\sqrt{\frac{C_{out}}{L_f}}$$

Fig. 20. By reorganizing the denominator under a normalized form, you can express a resonant frequency and a quality factor.

Unveiling The Zeroes

A zero in a transfer function corresponds to a root for which the numerator cancels, bringing a zeroed response magnitude at that particular frequency. Practically speaking, if we were to inject a sinusoidal stimulus tuned at a zero frequency, we would not observe an ac response in the output. With the FACTs, to identify zeroes in a circuit, we consider that the stimulus injected at the zero frequency is lost somewhere in the network, preventing the excitation from producing a response. In this mode, we say the response is *nulled*.

However, unlike classical harmonic excitation restricted to the imaginary axis $s=j\omega$, the FACTs conveniently consider the entire *s*-plane, meaning that our stimulus can take on negative frequency values. This abstraction nicely lets us identify networks which can shunt a given branch to ground when $s = s_z$ or become an infinite resistance when in series with the stimulus path. These two conditions bring a null in the output.

This is sometimes complicated to grasp for a student learning the FACTs and that is the reason why I have spent time documenting numerous examples in reference [12]. I invite the reader to look at this document should he want to acquire the skill.

Back to our circuit, what condition in Fig. 21 would induce a null on the output if we were to ac-modulate node *d*? If the series connection of r_C with C_{out} becomes a *transformed* short circuit, then we have an output null.

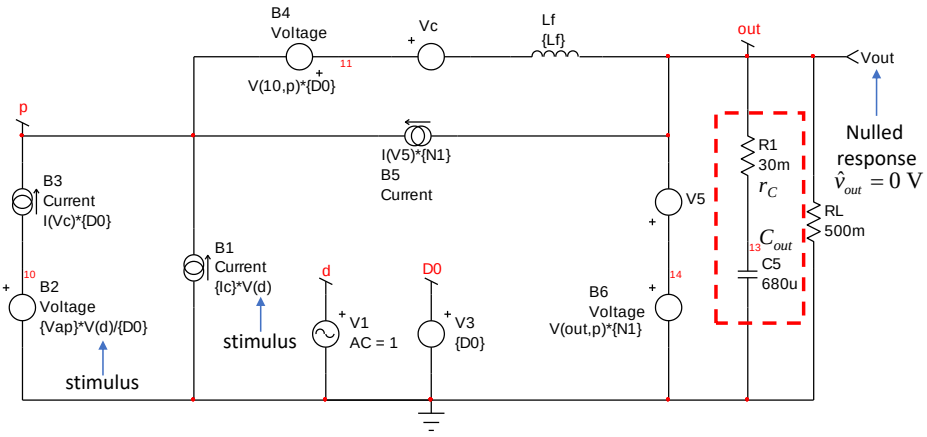

Fig. 21. If capacitor C_{out} and its parasitic resistance r_C become a transformed short circuit at a certain frequency, the response is nulled.

In the Laplace domain, it would imply:

$$r_C + \frac{1}{sC_{out}} = 0 \rightarrow s_z = -\frac{1}{r_C C_{out}} \qquad (30)$$

Bringing a first zero located at

$$\omega_{z_1} = \frac{1}{r_C C_{out}} \qquad (31)$$

For the second zero, I will resort to a so-called null double injection or NDI. In this mode, the stimulus is back (remember we zeroed it for determining the poles) and we install our test generator I_T across inductor L_f.

This time, we will determine the resistance $R = V_T/I_T$ when the response is nulled. In this mode, the ac output is 0 V and there is no current in R_{load}. It is not to be confused with a short circuit. The circuit is that of Fig. 22.

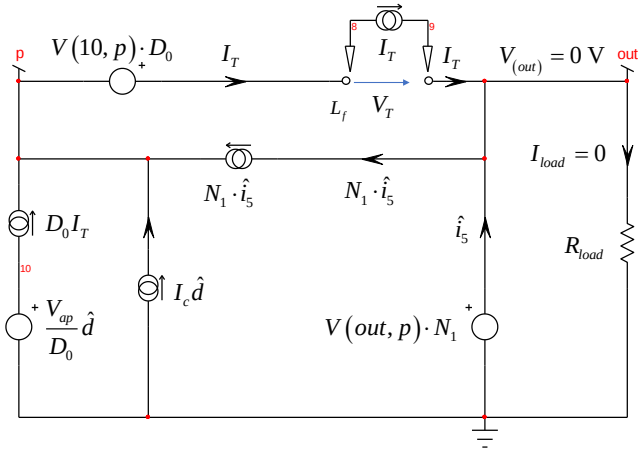

Fig. 22. In an NDI, the stimulus is back and I_T is adjusted to bring a null in the output voltage.

We first can write:

$$I_T = i_5\left(N_1 - 1\right) \tag{32}$$

Then, if the output node is nulled at 0 V, we have

$$V_{(p)} + V_{(10)}D_0 - V_{(p)}D_0 + V_T = V_{(out)} = 0 \tag{33}$$

The null appears across the low-side voltage source, therefore

$$V_{(out)}N_1 - V_{(p)}N_1 = 0 \tag{34}$$

Because V_{out} = 0 V, we can see that

$$V_{(p)} = 0 \tag{35}$$

From (33) with (35), we extract the voltage at node 10:

$$V_T = -V_{(10)}D_0 \tag{36}$$

We can also express V_T as

$$V_T = -\frac{V_{ap}}{D_0}D_0\hat{d} = -V_{ap}\hat{d} \tag{37}$$

Current I_T splits through different terms:

$$I_T = D_0 I_T + I_c\hat{d} + N_1 i_5 \tag{38}$$

From the above expression, I can define current i_5 as

$$i_5 = -\frac{D_0 I_T - I_T + I_c\hat{d}}{N_1} \tag{39}$$

which I can plug into (32) to obtain

$$I_T = -\frac{D_0 I_T - I_T + I_c\hat{d}}{N_1}\left(N_1 - 1\right) \tag{40}$$

I extract current I_T which is now defined by

$$I_T = \frac{I_c\hat{d} - I_c N_1\hat{d}}{D_0 N_1 - D_0 + 1} \tag{41}$$

Finally, by dividing (37) by (41), I obtain the wanted resistance R:

$$R = \frac{V_T}{I_T} = -\frac{V_{ap}\hat{d}}{\frac{I_c\hat{d} - I_c N_1\hat{d}}{D_0 N_1 - D_0 + 1}} = \frac{V_{ap}\left[D_0\left(N_1 - 1\right) + 1\right]}{I_c\left(N_1 - 1\right)} \qquad (42)$$

The second zero involving inductor L_f is thus defined as

$$\omega_{z_2} = \frac{R}{L_f} = \frac{V_{ap}\left[\left(N_1 - 1\right)D_0 + 1\right]}{I_c L_f\left(N_1 - 1\right)} \qquad (43)$$

When I determine a resistance in an NDI process, I like to validate the result with a SPICE simulation. In this mode, I use a voltage-controlled current source which injects a test current I_T and adjusts it for nulling the output. The example is illustrated in Fig. 23 where SPICE determines the dc operating point leading to a zeroed output voltage. Probing the node *Rzero* returns the value of the resistance $R = V_T/I_T$:

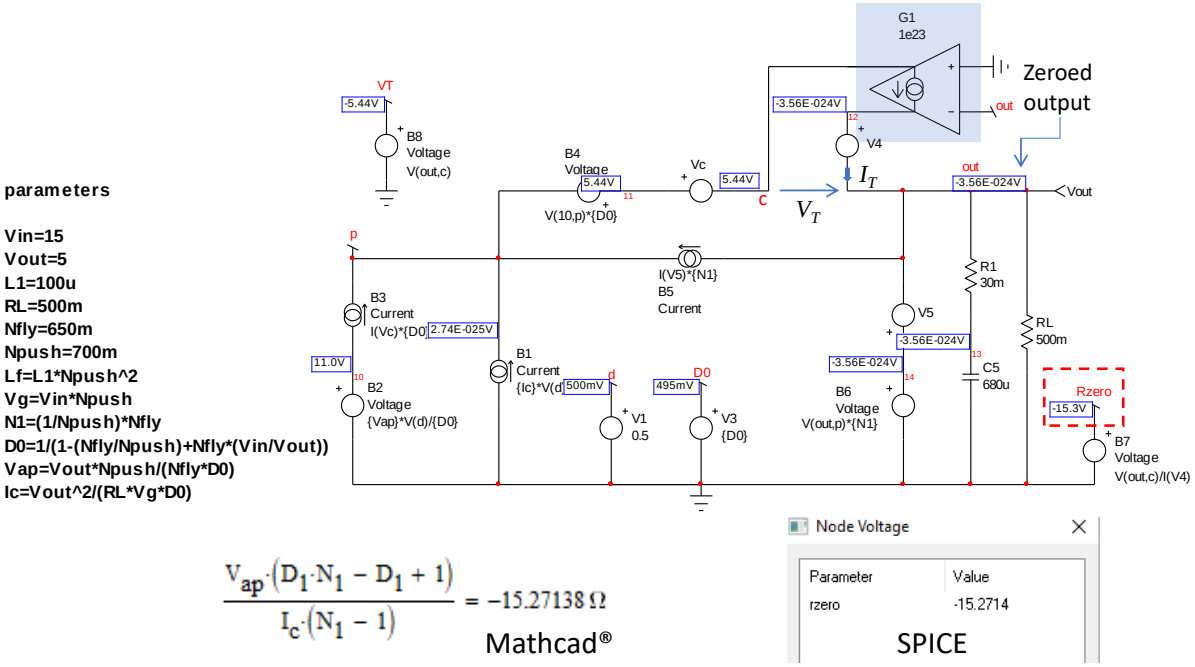

Fig. 23. A SPICE simulation is an excellent way to check the correctness of the results in a NDI exercise.

In this example, the resistance is negative and we have a right-half-plane zero. We could infer this result from (43) in which N_1 corresponds to the ratio N_{fly} over N_{push}. With the values adopted in this 5-V converter, the zero moves such that, if

- $N_{fly} < N_{push}$, ω_{z2} is a right-half-plane zero
- $N_{fly} = N_{push}$, ω_{z2} is pushed to infinity
- $N_{fly} > N_{push}$, ω_{z2} is a left-half-plane zero

The final transfer function can now be assembled by combining the poles, the zeroes and the quasi-static gain we have found in the beginning of this article:

$$H(s) = H_0 \frac{\left(1+\frac{s}{\omega_{z_1}}\right)\left(1+\frac{s}{\omega_{z_2}}\right)}{1+\frac{s}{\omega_0 Q}+\left(\frac{s}{\omega_0}\right)^2} \quad (44)$$

$$H_0 = \frac{1}{V_p} \frac{N_{fly} N_{push}{}^2 V_{in}}{\left[\left(N_{fly}-N_{push}\right)D+N_{push}\right]^2} \quad (45)$$

$$\omega_{z_1} = \frac{1}{r_C C_{out}} \text{ and } \omega_{z_2} = \frac{V_{ap}\left[\left(N_1-1\right)D_0+1\right]}{I_c L_f \left(N_1-1\right)} \quad (46)$$

$$\omega_0 = \frac{1}{\sqrt{\frac{L_f N_1{}^2}{R_{load}\left(D_0 N_1 - D_0 + 1\right)^2} C_{out}\left(r_C + R_{load}\right)}} \quad (47)$$

$$Q = \frac{\sqrt{\frac{L_f N_1{}^2}{R_{load}\left(D_0 N_1 - D_0 + 1\right)^2} C_{out}\left(r_C + R_{load}\right)}}{\frac{L_f N_1{}^2}{R_{load}\left(D_0 N_1 - D_0 + 1\right)^2} + r_C C_{out}} \quad (48)$$

Testing The Model

To check the control-to-output transfer function, I have collected magnitude and phase data coming from the SIMPLIS template of Fig. 9 and imported them into the Mathcad sheet, reproducing the same exact operating point and components values as shown in Fig. 24.

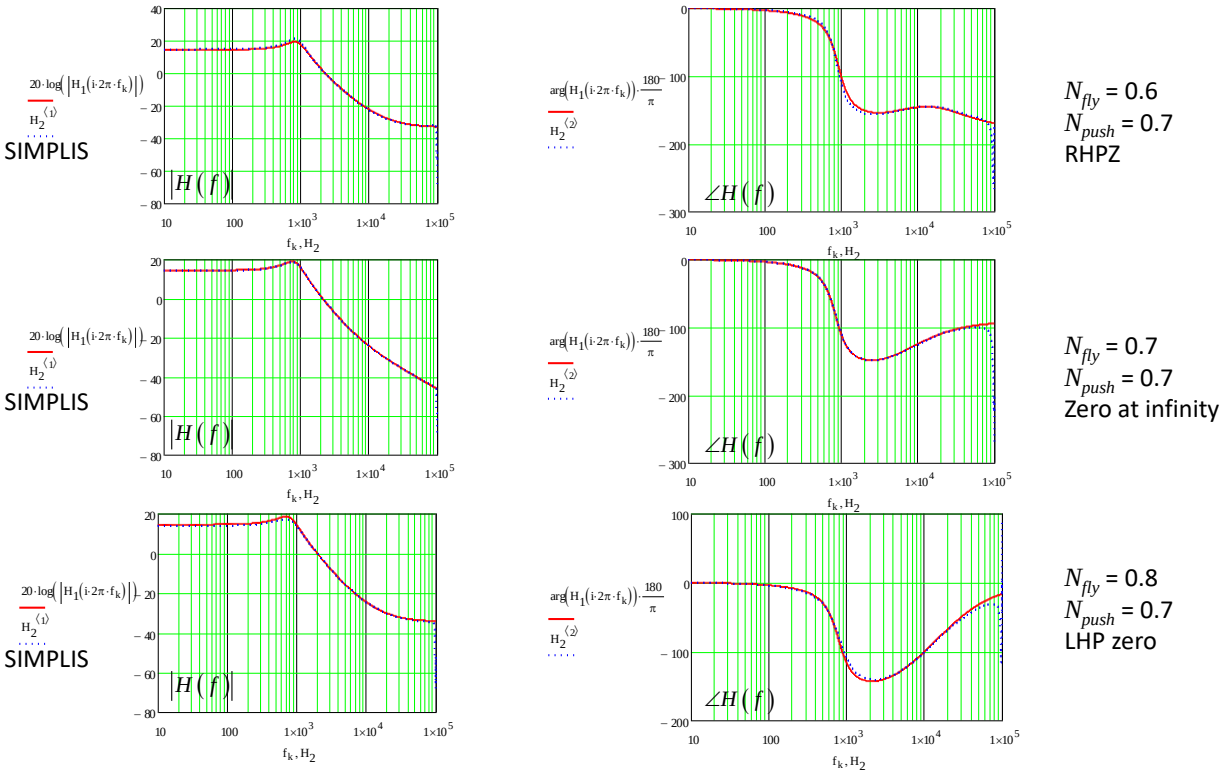

Fig. 24. The analytical response from Mathcad (solid lines in red) perfectly agrees with the ac response delivered by SIMPLIS (dotted lines in blue).

The magnitude and phase of both sources match very well with each other, illustrating the zero jumping from the left to the right half-plane in relationship with the transformers' turns ratios.

For those of you interested in checking the Weinberg SIMPLIS template, you can freely download my pack of 130+ ready-made templates from reference [13] which includes the voltage- and current-mode versions, as well as a SIMetrix averaged model.

Conclusion

This article details how I derived the control-to-output transfer function of the Weinberg converter operated in continuous conduction mode and in voltage mode. The PWM switch lends itself perfectly to small-signal modeling and it is the approach I have retained, despite the apparent complexity in revealing its presence through an equivalent circuit.

Once this equivalent, small-signal model is obtained, the fast analytical circuits techniques help deriving the position of poles and zeroes in a swift and efficient way. A simulation comparing the ac response obtained from a SIMPLIS simulation confirms the validity of the steps I have adopted in this process.

References

1. "A Boost Regulator with a new Energy-Transfer Principle" by Alan H. Weinberg, proceedings of the Spacecraft Power Conditioning Electronics Seminar, 1974.
2. "Small-Signal Modeling and Analysis of the Weinberg Converter for High-Power Satellites Bus Application" by W. Lei and Y. Li, Chinese Journal of Electronics, vol. 18, no. 1, January 2009.
3. "Analysis and Modeling of Weinberg Converter System with Output Current Limiter" by C-Y Hung, C.Q. Lee and H. Lee, IEEE Industry Applications Conference, Orlando, FL, USA, 1995.

4. "*Transfer Functions of Switching Converters*" by Christophe Basso, Faraday Press, June 2021.
5. "Active-clamp PWM converters: design-oriented analysis and small-signal characterization" by G. Stojcic, MS thesis, Virginia Polytechnic Institute and State University, June 1995.
6. "Optimum Topology High Voltage DC-to-DC Converter" by Gordon Bloom, U.S. patent 4,318,166, March 1982.
7. *Switching Power Supply Design,* 3rd edition by Abraham I. Pressman, Keith Billings and Taylor Morey, McGraw-Hill, 2009.
8. "Design of an All-SiC Parallel DC/DC Weinberg Converter Unit Using RF Control" by Sudip K. Mazumder, Kaustuva Acharya and Chuen Ming Tan, IEEE Transactions on Power Electronics, vol. 23, no. 6, November 2008.
9. "Simplified analysis of PWM converters using model of PWM switch. Continuous conduction mode" by Vatché Vorpérian, IEEE Transactions on Aerospace and Electronic Systems, vol. 26, no. 3, May 1990.
10. "Simplified analysis of PWM converters using model of PWM switch. Discontinuous conduction mode" by Vatché Vorpérian, *IEEE Transactions on Aerospace and Electronic Systems*, vol. 26, no. 3, May 1990.
11. "A Three-Day Course on a Circuit-Oriented Approach to the Analysis and Design of PWM dc-to-dc Converters using the Model of the PWM switch" by Vatché Vorpérian, in-house course, Toulouse, 2004.
12. *The Fast Track to Determining Transfer Functions of Linear Circuits: the Student Guide* by Christophe Basso Faraday Press, December 2023.
13. Download the free set of 130+ ready-made SIMPLIS templates from https://powersimtof.com/Downloads/Book/Christophe Basso SIMPLIS Collection.pdf.

About The Author

Christophe Basso is a business development manager with Future Electronics, a member of the power team and covering EMEA. Previously, he was a technical fellow with onsemi for 24 years where he originated numerous integrated circuits. SPICE simulation is also one of his favorite subjects and he has authored two books on the subject. Christophe's latest work is "An Intuitive Guide to Compensating Switching Power Supplies". Christophe received a BSEE-equivalent from the Montpellier University, France and an MSEE from the Institut National Polytechnique de Toulouse, France. He holds 25 patents on power conversion and often publishes papers in conferences and trade magazines.

For further reading on designing dc-dc converters, see the How2Power Design Guide, locate the "Power Supply Function" category and select "DC-DC converters".